

Fiber Spinning for Reducing Polarization Mode Dispersion in Single-Mode Fibers: Theory and Applications

Ming-Jun Li, Xin Chen and Daniel A. Nolan

Science and Technology Division, Corning Incorporated, SP-AR-02-2, Corning, NY 14831

Tel: 607-974-3099, Fax: 607-974-9271, E-mail: lim@corning.com

ABSTRACT

This paper surveys recent progress in fiber spinning technology for reducing polarization mode dispersion with the focus on theoretical understanding of fiber spinning mechanism and features of spun fibers, as well as their applications in fiber spin profiles designs. First, a brief introduction to the requirements of fiber PMD for high-speed optical fiber communications systems is given. Further discussion covers several spin technologies, including preform spinning and fiber spinning. Different theoretical approaches for modeling fiber spinning are reviewed with the emphasis on the coupled-mode formalism. The coupled-mode theory is then applied to different fiber spin profile designs, including constant, sinusoidal and frequency and amplitude modulated spin profiles. Main features of these spin profiles, such as PMD reduction dependence on fiber beatlength and sensitivity to spin parameters, are compared. Scaling properties of spun fibers, which show different behaviors from unspun fibers, are also discussed.

Keywords: polarization mode dispersion (PMD), fiber spinning, spun fiber, birefringence, coupled-mode theory, spin profile design, PMD scaling

1. INTRODUCTION

As optical transmission systems move towards higher bit rates, more wavelength channels and longer distances, various impairments from fiber chromatic dispersion, polarization mode dispersion (PMD) and non-linear effects are becoming limiting factors to the system performance. PMD arises from fiber imperfections, such as geometry and stress asymmetries, causing the two polarization modes to travel with different group velocities in a single-mode fiber. In digital transmission systems, PMD causes pulse splitting and pulse broadening, which limits the bit rate and the transmission distance [1]. Typical system tolerance to PMD is about 10% of one bit period. This translates to 40 ps for 2.5 Gb/s system, 10 ps for 10 Gb/s and only 2.5 ps for 40 Gb/s system. As the bit rate increases, the requirement for PMD becomes more stringent. For analog systems, PMD causes signal distortion [1]. For a 60-channel analog system, PMD has to be below 4 ps to guarantee the signal quality. It is therefore important to deploy low PMD fibers for both digital and analog systems.

In the past decade, significant efforts have been made to understand the PMD issues and to mitigate PMD effects in the systems. There are two ways to reduce fiber PMD. The first one is to minimize asymmetries in refractive index profile and stress [2-5]. This involves fiber manufacturing process improvements to ensure better fiber geometry and to reduce the stress level in the fiber. The second method is to introduce controlled polarization mode coupling by fiber spinning [6-19]. Fiber spinning has been used in fiber manufacturing since the early 1990s, and has proven to be an effective technique to reduce fiber PMD.

This paper intends to review recent progress in fiber spinning technology for reducing polarization mode dispersion. The focus will be on the theoretical understanding of fiber spinning mechanism and features of spun fibers, as well as applications in fiber spin profiles designs.

2. FIBER SPINNING TECHNOLOGIES

The concept of fiber spinning was originally proposed more than two decades ago in a paper published by Barlow et al. [6]. In that paper, the spun fiber was made by rotating the preform during the draw, as shown schematically in Figure 1 (a). In this approach, the fiber draw system is the same as the conventional system except that a rotating motor is placed

at the top of the preform. When the rotating motor is engaged with a predetermined speed, the preform turns around resulting in rotations of the fiber birefringent axes. The rotation is frozen into the fiber when it is cooled during the draw. This approach is straightforward and suitable for drawing fiber at low speed. However it is not suitable for fiber production with high-speed drawing because the motor has to rotate at a very high speed. To illustrate this, we consider a fiber spin rate of 3 turns/m. For a draw speed of 1 m/s, the preform rotation speed is only 180 RPM. However, for a modern draw tower running at greater than 20 m/s draw speed, the preform has to rotate at a speed of more than 3600 RPM, which is not practical. This is one reason why fiber spinning was not used in fiber production until the mid-1990s, when more practical spin methods were proposed. Another reason is that the systems at the time were deployed at low bit rates (≤ 2.5 Gb/s) and PMD was not a major issue then.

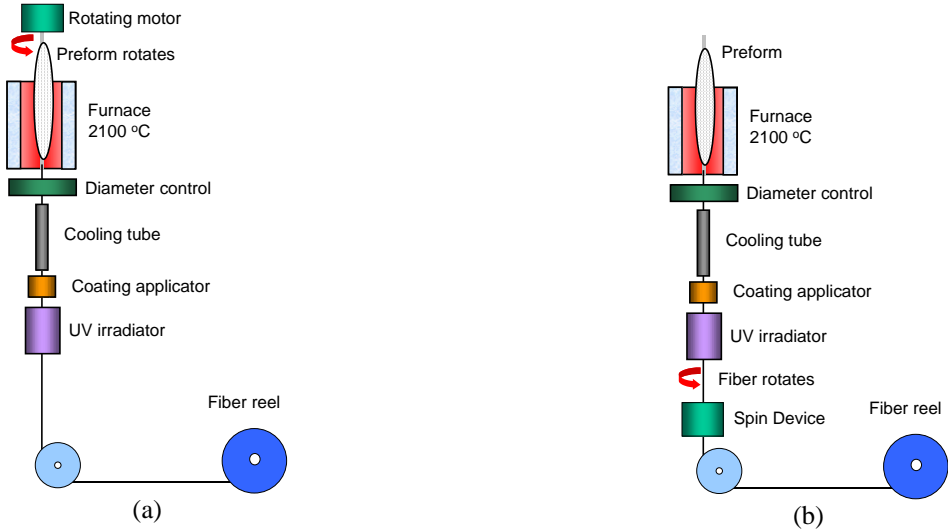


Figure 1: Two approaches to introduce fiber spin: (a) rotate the preform, (b) rotate the fiber directly.

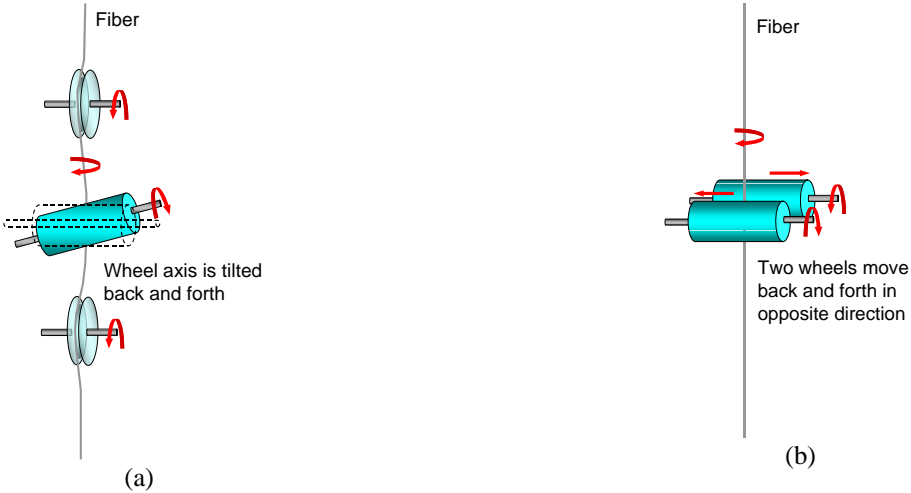


Figure 2: Examples of fiber spin device: (a) tilted wheel, (b) two moving wheels.

More practical techniques were proposed in the mid 1990s, for example, by Hart et al. [7] to spin the fiber directly instead of the preform. Over time, wider use of the fiber spinning technique was introduced in fiber production to make low PMD fibers. In this approach, as shown in Figure 1 (b), a fiber spin device is placed in the draw tower to rotate the fiber directly. Two examples of fiber spin device are illustrated in Figure 2. In the first example, shown in Figure 2 (a), a wheel is in contact with the fiber [7,8]. The wheel is tilted with respect to its horizontal position, which applies a torque

to rotate the fiber. In the second example, shown in Figure 2 (b), two wheels are placed horizontally and in contact with the fiber [8]. The two wheels move in opposite directions back and forth, causing the fiber to rotate. Spinning the fiber directly avoids the problem of high preform rotation speed. Furthermore, it provides flexibility to control and implement different spin profiles for better PMD reduction, which will be discussed in the next section of the paper.

3. FIBER SPIN THEORY

Two approaches for modeling PMD reduction by fiber spinning have been proposed. One approach is based on the evolution of the state of polarization [9,10]. In this approach, the evolution of polarization dispersion vector is governed by the dynamic equation that is related to the local birefringence vector. By solving the dynamic equation, the polarization dispersion vector is obtained, whose module gives the differential group delay (DGD). Another approach is based on Jones matrix coupled-mode theory [11]. In this approach, the complex amplitudes of the two polarization modes are described by the coupled-mode equations. By solving the coupled mode equations, the complex amplitudes are obtained and the Jones matrix is determined. The DGD can be calculated from Jones matrix. In principle, the two approaches yield equivalent results. In this paper, we adopt the Jones matrix formalism. Through this approach, simple analytical solutions are obtained and various properties and features in spun fibers are revealed. In this section we describe the coupled mode-theory in details.

3.1. Fiber birefringence and PMD

Consider a birefringent fiber that supports two polarization modes with propagation constants of β_1 and β_2 . The difference between the propagation constants of the two modes is defined as the fiber birefringence $\Delta\beta$:

$$\Delta\beta = \beta_2 - \beta_1 \quad (1)$$

The birefringence can be also described in terms of the beat length which is defined as

$$L_B = \frac{2\pi}{\Delta\beta} \quad (2)$$

The physical meaning of the beat length is that the polarization state of light is reproduced after traveling a distance of L_B . Due to the fiber birefringence, the two polarization modes propagate with different group velocities. The PMD γ_ω of a fiber at a position z in the fiber is defined as the differential group delay (DGD) between the two polarization modes in a unit length:

$$\gamma_\omega = \frac{d\Delta\beta}{d\omega} \quad (3)$$

where ω is the angular frequency of light. For a uniform birefringent fiber without random mode coupling, the total DGD after traveling a fiber is proportional to the fiber length L :

$$\tau = \gamma_\omega L \quad (4a)$$

The condition for which Eq. (4a) is valid is often referred to as the short fiber regime. However, for a long length of fiber with random perturbations, the DGD can not be calculated by a simple addition of local PMD. The coupled-mode equations and statistical tools must be used to find the total DGD. It has been found that the DGD scales with square root of fiber length with random coupling or in the long length regime:

$$\tau = \gamma_\omega \sqrt{h \cdot L} \quad (4b)$$

where h is the mode coupling length, which characterizes how frequent a mode coupling event happens in fibers. Since the birefringence in single-mode fibers used in telecommunications is normally small, the coupled-mode formalism based on perturbation theory can be used to describe different birefringence mechanisms in single-mode fibers [20,21], which includes birefringence due to fiber core deformation, stresses, bending, fiber spinning and twist, etc. In the remainder of this section, we review the coupled-mode theory and describe how to use it for different birefringence problems.

3.2. Coupled mode equations

The small birefringence of telecommunication fibers can be treated as an anisotropic perturbation to an originally isotropic material. Under the weakly guiding conditions, the electric field \mathbf{E} is described by the following wave equation [20]:

$$\Delta \mathbf{E} - \mu_0 \varepsilon_0 \varepsilon \mathbf{E} = \mu_0 \mathbf{p} \quad (5)$$

where ε_0 and μ_0 are the dielectric constant and the magnetic susceptibility of vacuum, respectively, ε is the relative dielectric constant of the unperturbed fiber, and \mathbf{p} is a perturbation term that is given by

$$\mathbf{p} = \varepsilon_0 \Delta \varepsilon \mathbf{E}, \quad (6)$$

where $\Delta \varepsilon$ is the dielectric tensor describing the anisotropy of the medium. Without the perturbation term, Eq. (6) has modal solutions of the following form

$$\mathbf{E}_n(x, y, z) = \mathbf{e}_n(x, y) \exp(-i\beta_0 z) \quad n = 1, 2 \quad (7)$$

where $\mathbf{e}_n(x, y)$ is the electric field distribution. For a single-mode fiber, $n=1, 2$, representing the two polarization modes.

Without any perturbation, the two modes are degenerate, and propagate with the same propagation constant β_0 . With the perturbation term, it is assumed that the electric field $\mathbf{E}(x, y, z)$ is given by a linear superposition of the two unperturbed modes:

$$\mathbf{E}(x, y, z) = \sum_n A_n(z) \mathbf{e}_n(x, y) \exp(-i\beta_0 z) \quad (8)$$

where $A_n(z)$ are complex coefficients describing the amplitudes and phases of the two modes \mathbf{E}_n . Substituting Eq. (8) into Eqs.(5-6), and using the orthogonality relation between the modes

$$\int \mathbf{e}_m(x, y) \cdot \mathbf{e}_n(x, y) dx dy = N_n \delta_{mn}, \quad (9)$$

and the weak-coupling condition

$$\frac{1}{\beta_0} \left| \frac{d^2 A_n}{dz^2} \right| \ll \left| \frac{dA_n}{dz} \right| \quad (10)$$

we get the coupled-mode equations that describe the evolution of the complex amplitudes $A_n(z)$:

$$\frac{d\mathbf{A}}{dz} = i\boldsymbol{\kappa} \cdot \mathbf{A} \quad (11)$$

where \mathbf{A} is the complex amplitude vector ,

$$\mathbf{A} = (A_1 \quad A_2)^T \quad (12)$$

and $\boldsymbol{\kappa}$ is the coupling coefficient matrix

$$\boldsymbol{\kappa} = \begin{pmatrix} \kappa_{11} & \kappa_{12} \\ \kappa_{21} & \kappa_{22} \end{pmatrix}. \quad (13)$$

The coupling coefficients are related to different types of perturbations:

$$\kappa_{nm} = \frac{k_0}{2n_0 N_0} \int \mathbf{e}_n^*(x, y) \cdot \Delta \varepsilon(x, y, z) \cdot \mathbf{e}_m(x, y) dx dy \quad n = 1, 2, \quad m = 1, 2 \quad (14)$$

where $k_0 = 2\pi/\lambda$ is the wave number in vacuum, n_0 is the effective refractive index of the unperturbed modes.

3.3. Jones matrix and fiber PMD

The local polarization evolution along a birefringent fiber is described by the coupled-mode equations. The overall polarization change after traveling through certain distance of the fiber is best described by a transform matrix called Jones matrix. Assuming that the loss of the fiber is negligible, the Jones matrix is unitary and has the following form

$$\mathbf{T} = \begin{pmatrix} u_1 & -u_2^* \\ u_2 & u_1^* \end{pmatrix} \quad \text{with} \quad |u_1|^2 + |u_2|^2 = 1 \quad (15)$$

The four complex elements of Jones matrix can be obtained by integrating the coupled mode equations with appropriate initial conditions. Once the Jones matrix is known, the PMD can be readily calculated from the matrix elements:

$$\tau = 2 \sqrt{\left| \frac{du_1}{d\omega} \right|^2 + \left| \frac{du_2}{d\omega} \right|^2} \quad (16)$$

To describe PMD reduction, we define a parameter called the PMD reduction factor (PMDRF) ζ as the ratio of DGD of spun fiber (τ) to that of unspun fiber (τ_0):

$$\zeta = \tau / \tau_0, \quad (17)$$

where the lengths of the spun and unspun fibers used in the calculation are the same. For example, when ζ is 1.0, no PMD reduction is achieved. When ζ is 0.5, a factor of two in PMD reduction is realized

3.4. Fiber configurations and coupling coefficients

The coupling coefficient matrix depends on the perturbation dielectric tensor, which has nine elements. The values of these elements are determined by the type of perturbation, i.e. the fiber configuration. In this section, we describe some fiber configurations that we are interested in and give their corresponding coupling coefficient matrices. It is worthwhile to note that the coupling matrices in this paper are expressed using the circular polarization basis, because it is more convenient to deal with fiber spinning-related problems.

A. Linear birefringent fiber

The linear birefringence is caused by perturbations such as core deformation, asymmetric lateral stresses, bending, etc. For linear birefringence, the coupling coefficient matrix is given by

$$\mathbf{\kappa} = \frac{1}{2} \begin{pmatrix} 0 & \Delta\beta e^{i2\phi} \\ \Delta\beta e^{-i2\phi} & 0 \end{pmatrix} \quad (18)$$

where $\Delta\beta$ is the linear birefringence, and ϕ is the orientation of the birefringence with respect to the x -axis.

B. Spun fiber

In a spun fiber, the birefringence orientation rotates with respect to the x -axis. The accumulated rotation angle ϕ is thus a function of the fiber length z , which is determined by the spin rate $\alpha(z)$:

$$\phi = \int_0^z \alpha(z) dz \quad (19)$$

Substituting Eq.(19) into Eq.(18), we get the coupling coefficient matrix for spun fiber:

$$\mathbf{\kappa} = \frac{1}{2} \begin{pmatrix} 0 & \Delta\beta e^{i2\int_0^z \alpha(z) dz} \\ \Delta\beta e^{-i2\int_0^z \alpha(z) dz} & 0 \end{pmatrix} \quad (20)$$

C. Twisted fiber

Twisting a fiber produces two effects: birefringence rotation and mechanical torsion. The birefringence rotation is similar to that of the spun fiber. If the twist rate is T , the angle ϕ is calculated by:

$$\phi = Tz \quad (21)$$

The torsion component is determined by the photo-elastic coefficients of fiber. The torsion stress produces circular birefringence that is proportional to the twist rate:

$$\delta = gT \quad (22)$$

Where g is a coefficient that is determined by the photo-elastic coefficients of glass. The typical value for silica fibers is 0.16. Combining the rotation and torsion effects, the coupling matrix is written in the form of

$$\mathbf{\kappa} = \frac{1}{2} \begin{pmatrix} \delta & \Delta\beta e^{i2Tz} \\ \Delta\beta e^{-i2Tz} & -\delta \end{pmatrix} \quad (23)$$

D. Fiber with Lateral Load

Applying lateral load force to a fiber produces linear birefringence on top of the intrinsic linear birefringence of the fiber. The coupling coefficient matrix of a fiber under the lateral load is expressed by the following equation:

$$\mathbf{\kappa} = \frac{1}{2} \begin{pmatrix} 0 & \Delta\beta e^{i2\phi} + \Delta\beta_p e^{i2\phi_p} \\ \Delta\beta e^{-i2\phi} + \Delta\beta_p e^{-i2\phi_p} & 0 \end{pmatrix} \quad (24)$$

where the subscript p denotes the perturbation introduced by the lateral load. The lateral load-induced birefringence depends on the differential stress $\Delta\sigma$ in the glass between the two directions that parallel and perpendicular to the load direction:

$$\Delta\beta_p = k_0 C \Delta\sigma \quad (25)$$

where k_0 is the wave number in vacuum, and C is the stress-optical constant. If we assume that the lateral load can be represented by two parallel plates that are compressed on the fiber, the differential stress in the glass is proportional to the lateral compression force per unit length F :

$$\Delta\sigma = qF \quad (26)$$

where q is a constant that depends on fiber coating types.

3.5. Solutions of the coupled equations

Generally, the coupling matrix is z -dependent, and analytical solutions of Eq. (11) do not exist in most cases. Numerical integration is often used to get numerical solutions. Different numerical methods, such as the finite difference method, Runge-Kutta method, can be applied to solve the coupled-mode equation. However in two special cases, we can derive analytical solutions, which will be discussed in this section.

A. Constant-rate spinning

For constant-rate spin, the spin function can be written as

$$\alpha = \alpha_0 \quad (27)$$

where α_0 is a constant. In this case, the fiber birefringence rates in one direction with a rate of α_0 . This is why constant-rate spinning is sometimes referred as unidirectional spinning. For a spun fiber with a constant spin rate, the integral in the coupling matrix of Eq.(19) can be calculated easily, and the coupled equation becomes

$$\frac{dA_1}{dz} = \frac{1}{2} i \Delta\beta e^{i2\alpha_0 z} A_2 \quad (28)$$

$$\frac{dA_2}{dz} = \frac{1}{2} i \Delta\beta e^{-i2\alpha_0 z} A_1 \quad (29)$$

with the initial conditions $A_1(0)=1$, $A_2(0)=0$. The solutions for Eqs. (28) and (29) are:

$$A_1 = -\frac{\alpha_0 - \nu}{2\nu} e^{i(\alpha_0 + \nu)z} + \frac{\alpha_0 + \nu}{2\nu} e^{i(\alpha_0 - \nu)z} \quad (30)$$

$$A_2 = \frac{\Delta\beta}{4\nu} e^{i(-\alpha_0 + \nu)z} - \frac{\Delta\beta}{4\nu} e^{-i(\alpha_0 + \nu)z} \quad (31)$$

where $\nu = \sqrt{\alpha_0^2 + \frac{1}{4} \Delta\beta^2}$.

Using Eqs.(15) and (16), we find that the DGD can be expressed by a simple formular for constant spinning:

$$\tau(z) = \frac{\gamma_\omega}{2\nu} \sqrt{(\Delta\beta)^2 z^2 + \left(\frac{4\alpha_0}{\Delta\beta} \sin\left(\frac{\Delta\beta z}{2}\right) \right)^2}. \quad (32)$$

The sinusoidal term does not play an important role when fiber length is sufficiently long. Thus in longer length, the DGD is,

$$\tau(z) = \frac{\gamma_\omega \cdot \Delta\beta \cdot z}{2\nu} \quad (33)$$

Eq. (33) indicates that the DGD scales linearly with the fiber length, and the PMDRF takes the form,

$$\zeta = \frac{\Delta\beta}{2\nu} \quad (34)$$

It is noticed that for constant-rate spun fibers, the PMDRF is dependent on the fiber beatlength or birefringence regardless what beatlength regime they are in or what spin rate is taken.

B. Periodic spin functions

For periodic spin functions, under certain conditions we can derive approximate analytical solutions using the perturbation theory [12]. With the initial conditions we have assumed in the previous section, the first-order perturbation solutions of $A_1(z)$ and $A_2(z)$ are:

$$A_1(z) = 1 \quad (35)$$

$$A_2(z) = (i/2)\Delta\beta \int_0^z \exp[-2i\Theta(z')]dz' \quad (36)$$

where $\Theta(z) = \int_0^z \alpha(z')dz'$. It is straightforward to obtain the DGD using Eq. (16),

$$\tau(z) = \gamma_\omega \left| \int_0^z \exp[-2i\Theta(z')]dz' \right|. \quad (37)$$

We have tested the validity of this solution. It is found that when the beatlength is longer than a few meters, i.e. $\Delta\beta \sim 1$, the first order perturbation theory is valid to a high degree. For sinusoidal types of spin profiles, a simple expression for the PMD reduction factor can be obtained from the perturbation solutions. Note that the sinusoidal spin profile takes the form,

$$\alpha(z) = \alpha_0 \cos(\eta z) \quad (38)$$

where α_0 is the spin magnitude, and η is the angular frequency of spatial modulations, which is linked to the spin period Λ in the form of $\eta = 2\pi/\Lambda$. The integration of the spin profile is $\Theta(z) = \alpha_0 \sin(\eta z)/\eta$. We then obtain the DGD using Eq.(37),

$$\tau(z) = \gamma_\omega \left| \int_0^z \exp\left[-i \frac{2\alpha_0 \sin(\eta z')}{\eta}\right] dz' \right| \quad (39)$$

The integral can be evaluated analytically by using the Identity,

$$e^{-ix \sin(\theta)} = J_0(x) + 2 \sum_{n=1}^{\infty} J_{2n}(x) \cos(2n\theta) - 2i \sum_{n=0}^{\infty} J_{2n+1}(x) \sin((2n+1)\theta) \quad (40)$$

Thus we have,

$$\tau(z) = \gamma_\omega \sqrt{R^2(z) + I^2(z)} \quad (41)$$

where

$$R(z) = J_0(2\alpha/\eta)z + \sum_{n=1}^{\infty} \frac{J_{2n}(2\alpha/\eta)}{\eta n} \sin(2n\eta z) \quad (42)$$

$$I(z) = \sum_{n=0}^{\infty} \frac{J_{2n+1}(2\alpha/\eta)}{\eta(2n+1)} \cos(2(n+1)\eta z) \quad (43)$$

When $J_0(2\alpha/\eta)$ is not zero, the dominant contribution is from the linear increase term of the above equation. Omitting the oscillating terms, the DGD expression is now

$$\tau(z) \approx \gamma_\omega |J_0(2\alpha_0/\eta)| z \quad (44)$$

Like the constant-rate spun fibers, without random perturbation, the DGD increases linearly with the fiber length. Thus the PMDRF takes a very simple form,

$$\zeta = |J_0(2\alpha_0/\eta)| \quad (45)$$

Eq. (45) indicates the PMD reduction factor is beatlength independent for sinusoidally spun fibers with beatlengths of a few meters or longer.

When $J_0(2\alpha/\eta) = 0$, the linear increase term disappears and the oscillation terms can not be neglected. In this case, the DGD oscillates between 0 and a maximum value and does not increase with the propagation distance. The condition where the optimum PMD is achieved is called phase matching condition, which will be studied further in the next section.

4. APPLICATIONS OF FIBER SPIN THEORY

4.1. PMD reduction of different spin profiles

A. Constant-rate spin

Using Eq. (34), PMDRF ζ as a function of spin rate for different beat lengths were calculated for constant-rate spin and are plotted in Figure 3 [11]. It can be seen that PMD is reduced monotonously as the spin rate increases. For the same spin rate, PMDRF ζ depends on fiber beat length. The longer the beat length is, the lower the PMD will be. For high PMD fiber (beat length < 1 m), high spin rate is required to reduce PMD to below 0.1 level.

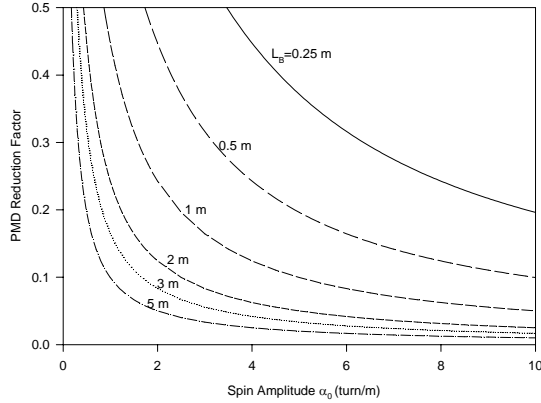


Figure 3: PMD reduction by constant rate spin for different fiber beat lengths.

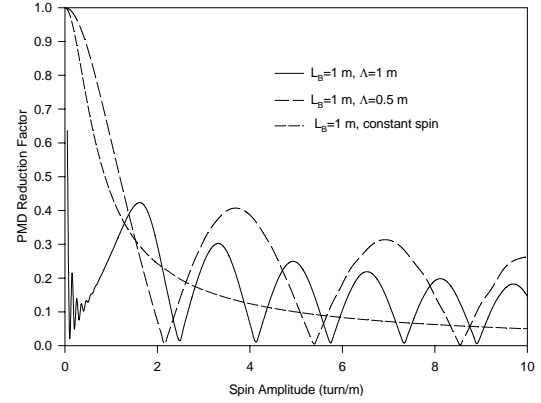


Figure 4: Example of PMD reduction by sinusoidal spins.

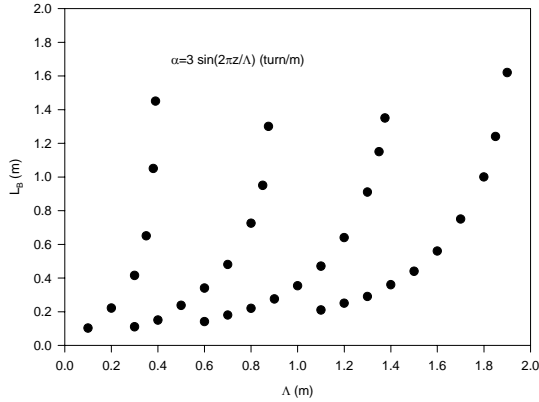


Figure 5: Phase matching diagram between fiber beat length and spin period.

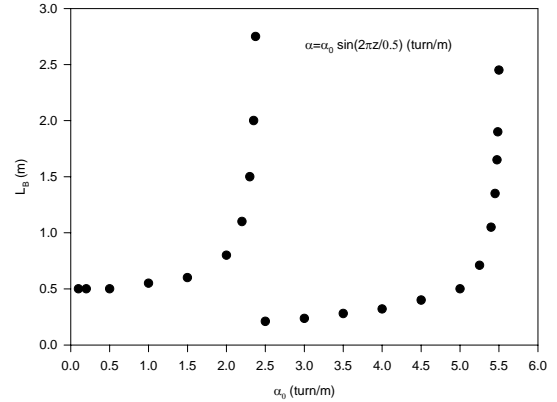


Figure 6: Phase matching diagram between fiber beat length and spin amplitude.

B. Sinusoidal spin

In Figure 4, we use beat length of 1 m as an example to illustrate PMD reduction by sinusoidal types of spin [11]. For comparison purposes, in Figure 4 we also show a curve of PMD reduction of constant spin rate. Figure 4 shows that, for sinusoidal types of spin, the PMDRF ζ oscillates with spin amplitude, which is different from the constant-rate spin. Figure 4 indicates that in a sinusoidal spin, phase matching can happen to result in low PMD, while in a constant spin, phase matching does not exist. The phase matching phenomenon can be explained by mode coupling mechanism. Constant spin reduces the fiber birefringence, but does not cause any mode coupling. For sinusoidal spin, the change in spin rate causes the two polarization modes to couple to each other, resulting in PMD compensation. For certain spin profiles and fiber birefringence, phase matching conditions are satisfied and maximum energy exchange occurs to

produce the best PMD reduction. The modeling results indicate that the phase matching depends on fiber beat length, spin period and spin amplitude. Figure 5 shows phase matching conditions between the fiber beat length and the spin period for a sinusoidal spin with the spin amplitude of 3 turn/m. Figure 6 shows phase matching conditions between the fiber beat length and the spin amplitude for a sinusoidal spin with the spin period of 0.5 m. We can see that, in Figures 5 and 6, for the beatlength longer than 1.2 m, the phase matching does not depend on beatlength. This means that we can use the same spin function to achieve very low PMD reduction for long beatlengths. However for shorter beatlengths, the phase matching has strong beatlength dependence. Because the birefringence of practical fibers is not constant and changes in an unpredictable manner, it is impossible to have phase match for all birefringence using only one sinusoidal spin in the short beatlength region. This problem can be resolved by designing spin profiles with many Fourier components. To achieve this, we developed the concept of using frequency and amplitude modulated spins.

C. Frequency and amplitude modulated spin

One way to increase the number of Fourier components is to use frequency modulated (FM) and amplitude modulated (AM) spin functions [11]. Examples of PMD reduction using FM and AM spins are given in Figure 7 together with constant and sinusoidal types of spin. The spin function used for the FM spin is as follows

$$\alpha = \alpha_0 \sin\{2\pi[f_0 + f_m \sin(2\pi z / \Lambda)]\} \quad (46)$$

where the amplitude $\alpha_0=3$ turns/m, the center frequency $f_0=5$ m⁻¹, the modulation frequency $f_m=4$ m⁻¹, and the modulation period of 5 m. The spin function of the AM spin is

$$\alpha = [\alpha_0 \sin(2\pi z / \Lambda_m)] \sin(2\pi z / \Lambda) \quad (47)$$

with the amplitude $\alpha_0=3$ turns/m, the modulation period $\Lambda_m=5$ m, and the spin period $\Lambda=0.5$ m. Compared to the constant and sinusoidal spin, the FM and AM spins produce much better PMD reduction in a broad band of fiber birefringence, because phase matched or nearly matched mode couplings are always achieved.

It is instructive to analyze the amount of mode coupling that occurs as light travels through three sections of fiber, an unspun section followed by a spun section and another unspun section. Figure 8 shows the amount of light that has coupled from the fast axis in the initial section to the fast axis in the final section after traversing the spun section. The length of the spun section and its 'unspun' beat length were chosen to be one meter. The plot shows that for certain spin rates, significant mode coupling and therefore significant mode delay compensation can occur. For other spin rates, little mode coupling and subsequently little mode delay compensation occurs. In a similar manner PMD resonances occur for sinusoidal spins as a function of the spin rate amplitude.

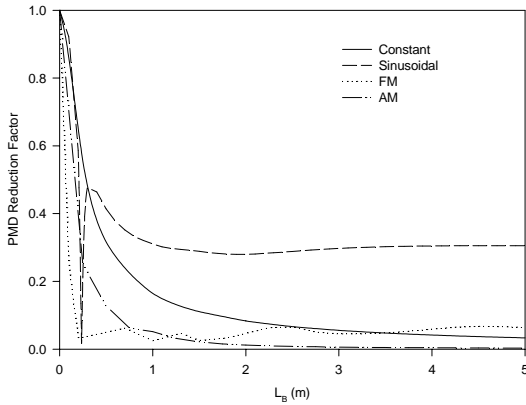


Figure 7: Comparison of constant, sinusoidal, frequency modulated and amplitude modulated spins.

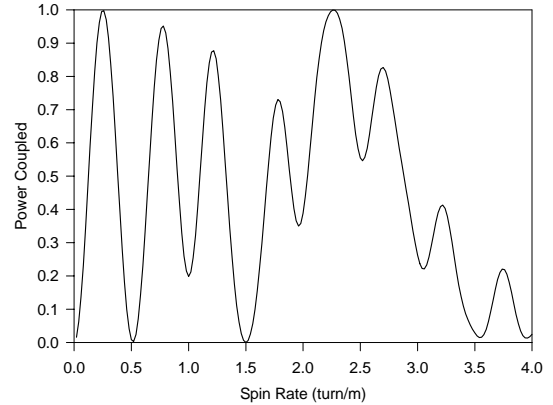


Figure 8: Mode coupling as a function of spin rate

4.2. Effects of residual stress on PMD

In the fiber spinning process, the fiber is rotated around its central axis by a torsional force applied to the fiber. The rotation is frozen into the fiber when it is cooled down, causing the fiber birefringent axes rotating along the fiber. In this process, a small amount of residual torsional stress is inevitably frozen into the fiber. However, in analyzing spun fibers, it is normally assumed that the spinning does not introduce any torsional stress in fiber for simplicity. This assumption is

valid only when the fiber intrinsic birefringence is much bigger than the birefringence induced by the residual torsional stress. With the improvement in fiber manufacturing technology in the past a few years, the fiber intrinsic birefringence has become much lower. For low intrinsic birefringent fibers, even a small amount residual stress is expected to contribute significantly to the total PMD. However, the impact of the residual stress on fiber PMD has not been well understood yet. In this section we study effects of residual stress on fiber PMD reduction of spun fibers using the coupled-mode theory [19].

Using the circular polarization mode basis, the coupling coefficient matrix of a spun fiber with residual torsional stress is expressed by the following equation:

$$\kappa = \frac{1}{2} \begin{pmatrix} \delta(z) & \Delta\beta_0 e^{2i \int \alpha(z) dz} \\ -2i \int \alpha(z) dz & -\delta(z) \\ \Delta\beta_0 e & 0 \end{pmatrix} \quad (48)$$

where $\Delta\beta_0$ is the intrinsic linear birefringence, $\alpha(z)$ is the spin function, and $\delta(z)$ is the circular birefringence induced by the residual stress due to fiber spinning, which is proportional to the spin rate:

$$\delta(z) = r_s g \alpha(z) \quad (49)$$

where g is a constant related to photo-elastic coefficients of glass, r_s is a factor that describes how much residual stress is frozen in the fiber. When $r_s = 1$, Eq.(48) represents the circular birefringence induced by pure mechanical twist of the fiber after the fiber drawing. In our analysis, we varied the residual stress factor r_s between 0 and 14%.

We study first the unidirectional spinning by increasing the fiber intrinsic beatlength from 1 to 100 m. It is found if the fiber beatlength is shorter than 5 m, the residual stress has negligible effects on the PMD. When the intrinsic fiber beatlength is longer than 5 m, the residual stress starts to show effects on the PMD. The stress effect becomes more pronounced when the intrinsic fiber beatlength gets longer. As an example, Figure 9 shows the PMDRF change as a function of spin amplitude for constant spinning. The intrinsic fiber beatlength in this figure is 50 m. It can be seen that for spin amplitudes less than 0.5 turns/m, the effect of residual stress is very small. When the spin amplitude increases, the PMDRF becomes bigger with the presence of residual stress, which is in contrast to the case without residual stress. For the same spin amplitude, the PMDRF increases with the residual stress level.

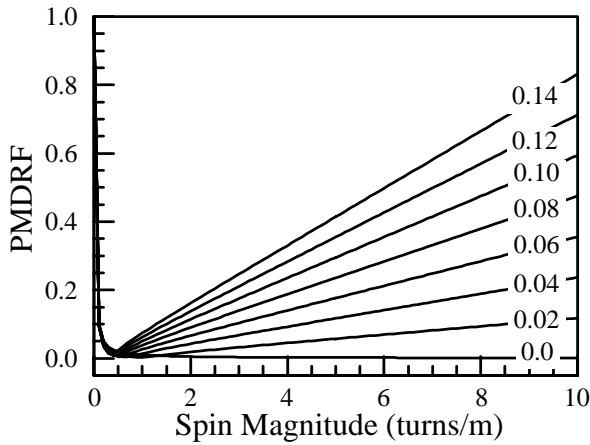


Figure 9: PMDRF change with spin amplitude for a unidirectional spun fiber. The beatlength is 50 m.

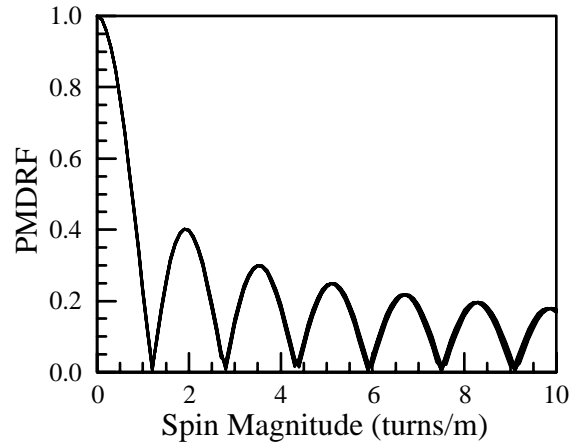


Figure 10: PMDRF change with spin amplitude for a sinusoidal spun fiber. The beatlength is 50 m. The spin period is 1 m.

On the other hand, the bidirectional spinning has a very different response to the residual stress. Numerical results show that the residual stress does not affect the PMDRF for bidirectional spun fibers. For example, in Figure 10, we plot the PMDRF as a function of spin amplitude for different residual stress levels for a sinusoidal spun fiber with 50 m intrinsic

fiber beatlength. The lines for different stress levels are almost identical, which means that the sinusoidal spinning is not sensitive to the residual stress.

The difference in response to the residual stress between the unidirectional and bidirectional spinning can be understood by examining residual stress evolution along the fiber. For unidirectional spin, Eq.(49) tells us that the stress is a constant for a constant spin amplitude. The stress effect accumulates linearly along the fiber, which contributes to the overall fiber PMD. For a sinusoidal spinning, the stress oscillates between a positive and negative value. The integration of the stress along the fiber is zero, which does not contribute to the overall fiber PMD.

4.3. Effects of lateral load and external twists on spun fibers

In this section, we show numerical results of PMD changes due to the lateral external twist for spun and unspun fibers [14]. In the calculation, the intrinsic fiber birefringence is assumed to have a beat length of 6 m. For unidirectional spun fibers, the spin rate is 4 turns/m. For bidirectional spun fibers, the spin rate is a sinusoidal function with the amplitude of 4 turns/m and a period of 1.2 m.

Figure 11 compares PMD changes of an unspun fiber and a bidirectional spun fiber due to lateral load. For the unspun fiber ($\alpha=0$) without external twist ($T=0$), the PMD change depends on the angle ϕ_p of the lateral load relative to the x -axis. If the lateral load is aligned with the intrinsic birefringence ($\phi_p=0^\circ$), the PMD increases linearly with the load force. If the lateral load is perpendicular to the intrinsic birefringence ($\phi_p=90^\circ$), the two effects cancel each other. After the intrinsic birefringence is canceled completely, the PMD starts to increase with the lateral load. For other angles, the PMD change is between the 0° and 90° lines. On the other hand, for the bidirectional spun fiber, because the orientation of the intrinsic birefringence rotates periodically with the spin rate, the PMD change due to the lateral load is independent of the load orientation. The behavior of unidirectional spun fiber is similar to that of bidirectional spun fiber.

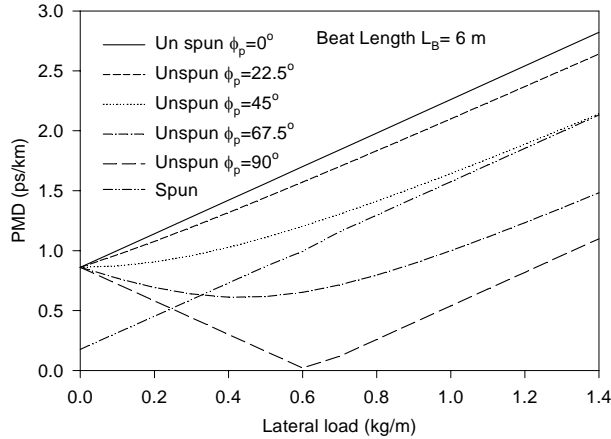


Figure 11. Calculated PMD changes as a function of lateral load for spun and unspun fibers.

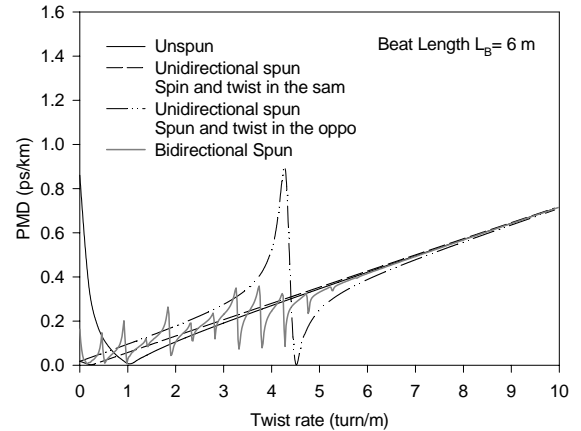


Figure 12. Calculated PMD changes as a function of external twist for spun and unspun fibers.

The external twist has two effects on PMD. First, it introduces wavelength independent mode coupling between the two polarization modes, which reduces the PMD in a way similar to the fiber spinning. Second, the twist induces a circular birefringence through the photo-elastic effect. The PMD produced by this circular birefringence is in opposite sign to that produced by the fiber linear birefringence. The PMD responses to the external twist are very different for spun and unspun fibers as shown in Figure 12. For the unspun fiber, the PMD is reduced first to zero by the twist, where the twist induced circular birefringence cancels the fiber linear birefringence completely. Then the PMD increases linearly with the twist rate due to the circular birefringence.

In Figure 12, the PMD response of the spun fibers to the external twist is more complicated, and the unidirectional and bidirectional spun fibers have different behaviors. For the unidirectional spun fiber, the PMD change depends on the twist direction relative to that of the fiber spin. If the twist is in the same direction as the spin, the twist enhances the PMD reduction at first, then increases the PMD when the twist induced circular birefringence gets larger than the linear birefringence. If the twist is in the opposite direction to the spin, it increases the PMD by compensating the spin effect when the twist rate is smaller than the spin rate. When the twist rate is equal to the spin rate, the spin effect is canceled completely by the twist, and the PMD reaches its peak value. If the twist rate is increased further, the PMD starts to decrease. After it reaches zero, the PMD increases linearly with the twist rate due to the circular birefringence. For the bidirectional spun fiber, the PMD fluctuates with the twist rate if the twist rate is smaller than or comparable to the spin amplitude. When the twist rate is much bigger than the spin amplitude, the PMD increases with the twist rate in a fashion similar to an unspun fiber.

4.4. PMD scaling properties of spun fibers

As mentioned in previous sections, spun fibers follow a linear scaling rule without random mode coupling or in the short length regime. When random mode coupling is present, it has been found that spun fibers follow a square root scaling rule similar to unspun fibers, but with a different rate depending on spin parameters [15]. The random mode coupling can be characterized by a random change of fiber birefringence axis and (or) a phase shift induced by external stress with a frequency of the occurrence of $1/h$, where h is called the mode-coupling length. Thus a fiber of length l can be divided into $[l/h]$ segments. Using this model, for a sinusoidally spun fiber under non-optimum conditions (no phase-matching), the DGD can be expressed in a simple form

$$\tau = \zeta \cdot \gamma_{\omega} \cdot \sqrt{hl} \quad (50)$$

Note that because the PMDRF ζ is independent of the fiber beatlength when the beatlength is greater than a few meters as discussed in Section 3.5.B, the DGD in the long length regime and in the presence of random mode coupling is corrected by a factor of ζ , which is the reduction introduced by fiber spinning during the fiber drawing process. In this case, the scaling property is similar to that of the linear birefringent fiber.

The simple scaling rule in Eq. (50) has been verified by using direct numerical modeling. Figure 13 shows the results of numerical simulation for a sinusoidally spun fiber under non-optimal conditions. The theoretical prediction based on Eq.(50) is also plotted using solid curve. As shown in Figure 13, the numerical modeling agrees with the theoretical prediction very well.

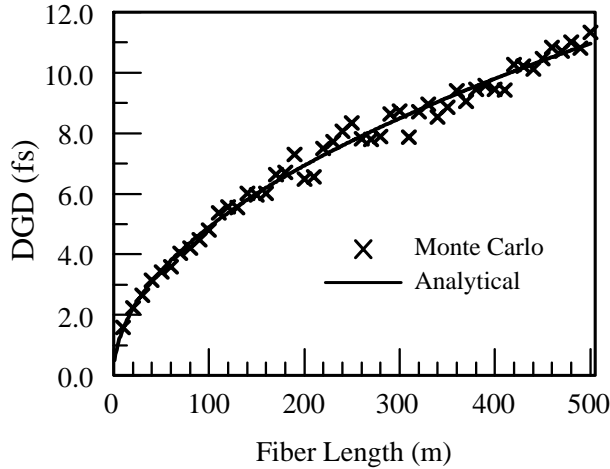


Figure 13. DGD of a spun fiber as a function of fiber length. Spin magnitude is 3.5 turns/m, spin period is 1.0m, fiber beatlength is 10.0m, and mode-coupling length is 10.0m.

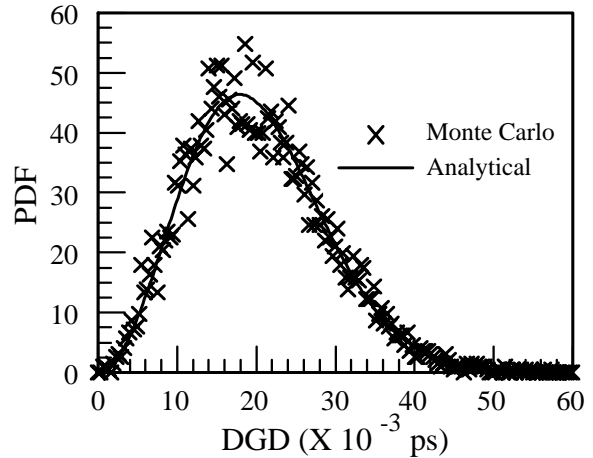


Figure 14. PDF as a function of DGD for a non-optimal spun fiber. Spin magnitude is 3.5 turns/m, spin period is 1.0m, mode coupling length is 10.0 m, and fiber length is 500m.

For unspun fibers with random mode coupling length of h , it is well known that the distribution of fiber DGD is Maxwellian:

$$P(\tau, z) = \frac{2\tau^2}{\sqrt{\pi}\sigma} \exp\left[-\frac{\tau^2}{2\sigma^2}\right] \quad (51)$$

where parameter σ is linked to the quadrature average of fiber DGD,

$$\sigma = (\lambda/cL_b)\sqrt{h \cdot l}/\sqrt{3} \quad (52)$$

It has been found that Maxwellian distribution also holds for spun fibers, except the parameter σ should be corrected by the contribution from fiber spinning. Thus the modified parameter σ now is,

$$\sigma = |J_0(2\alpha_0/\eta)| \cdot (\lambda/cL_b)\sqrt{h \cdot l}/\sqrt{3}. \quad (53)$$

This equation has been tested using Monte Carlo simulation. In Figure 14 we show the PDF as a function of fiber DGD obtained both from numerical calculations and Eq.(51). The numerical results are obtained over 6,000 randomly generated instances. It is found that the two agree very well.

When phase matching conditions are satisfied, the fiber is a periodic function, and it oscillates back and forth between 0 and a maximum value ε_{max} . Thus the DGD of one segment of fiber of length h is related to an average of the DGD within one spin period. Thus in the long length regime ($l \gg h$), the total DGD can be written as,

$$\tau = \varepsilon' \varepsilon_0 \sqrt{l/h} \quad (54)$$

where ε_0 is the quadrature average DGD within one spin period, and ε' is an coefficient that depends on the average coupling coefficient between two segments. For a phase-matching condition when $\alpha_0 = 2.76$ turns/m and $\eta = 2\pi \text{ m}^{-1}$, ε' is found to be 1.194. Another novel property here is that the DGD will increase when the mode-coupling length is shortened. This is understandable, since under optimal conditions the DGD is the minimum. Any perturbation will move the fiber away from the optimum conditions, causing PMD increase.

Although the DGD of optimized spun fibers scales with the coupling length differently from the DGD of non-optimized spun fibers, the DGD still follows the Maxwellian distribution in Eq. (51), but with a modified σ parameter

$$\sigma = \varepsilon' \varepsilon_0 \sqrt{l/h}/\sqrt{3} \quad (55)$$

Also, this equation has been verified by numerical Monte Carlo simulation.

5. CONCLUSIONS

Fiber spinning is an effective and practical way to produce low PMD fibers. Fiber spinning can be achieved by spinning the preform or by spinning the fiber directly during the fiber draw process. The latter is more suitable for high-speed industrial fiber manufacturing. Theoretical approaches for analyzing spun fibers have been developed. Among them, the coupled mode theory has been proven to be a very powerful tool. Great progress has been made to understand the effects of different spin profiles on PMD reduction and spun fiber properties. However, further studies are anticipated to fully understand all the aspects of spun fibers and to optimize the spin process.

REFERENCES

- 1 C.D. Poole, and J. Najel, "Polarization Effects in Lightwave Systems", in Optical Fiber Telecommunications IIIA, Edited by I.P. Kaminow and T.L. Koch, Academic Press, 1997, pp114-161.
- 2 A.M. Vengsarkar, L.G. Cohen, W.L. Mammel, "Theoretical Analysis, of Highly Elliptical – Core Fibers with arbitrary refractive Index Profile", Optics Letters, vol.17 1658 – 1660, 1992.
- 3 D.Q. Chowdhury, and D.A. Nolan, "Perturbation Model for computing optical fiber birefringence from two-dimensional refractive index profile", Optics Letters, vol.20, pp.1973 – 1975, 1995.
- 4 D.Q. Chowdhury and D. Wilcox, "Comparison between optical fiber birefringence induced by stress-anisotropy & geometric deformation", OFC/IOOC '99, Technical Digest, Vol 2 Page(s): 220 -222, 1999.
- 5 M. Fontaine, B. Wu V.P. Tzolov, W.J. Bock, and W. Ubranczyk, "Theoretical and experimental analysis of thermal stress effects on modal polarization properties of highly birefringent optical fibers", J. of Lightwave Technology, vol.14, pp. 585 – 591, 1996.
- 6 A. J. Barlow, J. J. Ramskov-Hansen, and D. N. Payne, "Birefringence and polarization mode-dispersion in spun single-mode fibers", Appl. Opt., vol. 20, 2963, 1981.

- 7 A. C. Hart, Jr., R. G. Huff, and K.L.Walker, "Method of making a fiber having low polarization mode dispersion due to a permanent spin," U.S. patent 5,298,047, March 29, 1994.
- 8 P.E. Blaszyk, W.R. Christoff, D.E. Gallagher, R.M. Hawk, and W.J. Kiefer, "Method and Apparatus for Introducing Controlled Spin in Optical Fibers", U.S. patent 6324872 B1, December 4, 2001.
- 9 R. E. Schuh, X. Shan, and A. S. Siddiqui, "Polarization mode dispersion in spun fibers with different linear birefringence and spinning Parameters", J. Lightwave Technol., vol.16, 1583, 1998
- 10 A. Galtarossa, Luca Palmieri, and Anna Pizzinat, "Optimized spinning design for low PMD fibers: an analytical approach", J. Lightwave Technol., vol. 19, 1502, 2001.
- 11 M.J.Li and D. A. Nolan, "Fiber spin-profile designs for producing fibers with low polarization mode dispersion", Optics Letters, vol.23, 1659-1661, 1998.
- 12 X. Chen, M. J. Li and D. A. Nolan, "Polarization mode dispersion of spun fibers: an analytical solution", Optics Letters, vol.27, 294-296, 2002.
- 13 R.E.Schuh, E.S.R. Sikora, N.G.Walker, A.S.Siddiqui, L.M.Gleeson and D. H. O. Bebbington, "Theoretical analysis and measurement of effects of fibre twist on polarization mode dispersion of optical fibres", Electron. Lett. , vol. 31, 1772-1773, 1995.
- 14 M. J. Li and A. F. Evans, D. W. Allen, and D. A. Nolan "Effects of lateral load and external twist on polarization-mode dispersion of spun and unspun fibers", Opt. Lett., vol. 24 1325, 1999.
- 15 X. Chen, M.-J. Li and D. A. Nolan, "Scaling properties of polarization mode dispersion of spun fibers in the presence of random mode coupling", Optics Letters, vol. 27, 1595, 2002.
- 16 Andrea Galtarossa, Paola Griggio, Anna Pizzinat, Luca Palmieri, "Calculation of the mean differential group delay of periodically spun, randomly birefringent fibers", Optics Letters, vol. 27, 692-694, 2002.
- 17 A. Pizzinat, B. S. Marks, L. Palmieri, C. R. Menyuk, A. Galtarossa, "Polarization mode dispersion of spun fibers with randomly varying birefringence", Optics Letters, vol. 28, 390-392, 2003.
- 18 D. Sarchi, and G. Roba, "PMD mitigating through constant spinning and twist control: experimental results", OFC'2003 Technical Digest, paper WJ2, pp.367-368, 2003.
- 19 M.J. Li, X. Chen, and D.A. Nolan, "Effects of Residual Torsional Stress on PMD of Spun Fibers", ECOC'2003.
- 20 R. Dandliker, "Rotational effects of polarization in optical fibers", in Anisotropic and Nonlinear Optical Waveguides, Edited by C.G. Someda, and G. Stegeman, Elsevier, New York, 1992, pp. 39-76.
- 21 D. Marcuse, Theory of Dielectric Optical Waveguides, Academic Press, Inc., Boston, 1991.